J|A|C|S
ARTICLES
Published on Web 01/16/2004

A Hexa-*peri*-hexabenzocoronene Cyclophane: An Addition to the Toolbox for Molecular Electronics

Mark D. Watson,*[,†,§] Frank Jäckel,[‡] Nikolai Severin,[‡] Jürgen P. Rabe,*[,‡] and Klaus Müllen*[,†]

Contribution from the Max-Planck-Institute for Polymer Research, Postfach 3148, D-55021 Mainz, Germany, and Department of Physics, Humboldt University Berlin, Newtonstrasse 15, D-12489 Berlin, Germany

Received July 24, 2003; E-mail: muellen@mpip-mainz.mpg.de; rabe@physik.hu-berlin.de

Abstract: Cyclophanes with the largest-to-date polycyclic aromatic hydrocarbon (hexa-*peri*-hexabenzocoronene, HBC) to be entrained in such a structural motif are reported. The two disks are covalently captured by intermolecular ring-closing olefin metathesis of dienes in good yield. DSC, optical microscopy, and WAXD show the new cyclophanes to self-assemble to thermotropic columnar liquid crystal mesophases similar to monomeric analogues. Solution spectroscopic studies reveal that the two disks within a single unit lie face-to-face, with a small average lateral offset. Self-assembly into two-dimensional crystals at a solid−liquid interface was visualized by STM, and the electrical properties of single molecules were assessed by scanning tunneling spectroscopy revealing a diode-like behavior which is similar to that previously reported for single HBC disks, laying the groundwork for future electrical interrogations of dynamic molecular complexes.

Introduction

Substituted monomeric hexa-*peri*-hexabenzocoronenes (HBCs) (**1**, R = flexible group) self-assemble in a face-to-face manner to form columnar stacks with requisite nanophase separation of the side chains. This leads to highly cohesive thermotropic columnar mesophases[1] persisting to above 400 °C and to aggregation in normal organic solvents well below micromolar concentrations.[2] The tendency to aggregate in solution is exploited here to covalently capture dimeric aggregates (target cyclophanes **4a**,**b**) in good yield under moderate dilution. The substantial magnetic anisotropy of the aromatic cores makes NMR a sensitive probe of local environments due to strong (de)shielding.[3] Standard solution spectroscopic methods thus sufficed to elucidate the intramolecular cofacial arrangement within these cyclophanes and to disclose subtle structural effects on molecular geometry. Both the inter- and the intramolecular stacking of disk segments into columns as well as the packing of the columns themselves in the solid state is revealed from wide-angle X-ray diffraction (WAXD).

Given that single HBC disks (**1b**) have previously been shown to cause diode-like behavior when completing the circuit between an STM tip and highly oriented pyrolytic graphite (HOPG),[4] these new cyclophanes with two disks in series present an interesting addition to the nano-toolbox for future molecular scale electronics. STM investigations of these new molecules in oriented monolayers at the interface between an organic solution and the basal plane of graphite reveal packing patterns which are sufficiently stable to allow for scanning tunneling spectroscopy (STS) experiments through two HBC disks in series within an environment of alkyl chains. This is the prerequisite to compare for the first time, to the best of our knowledge, current−voltage characteristics (I−V's) through single molecules and molecular double stacks of the same molecular species.

Molecular Formula

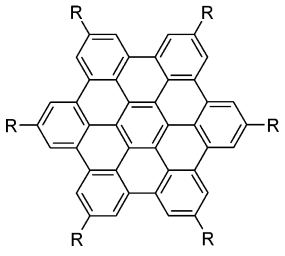

	R
1a	H
1b	n-$C_{12}H_{25}$
1c	3,7-dimethyl octanyl

Results

Synthesis. HBC diene **3** could be prepared in near quantitative yield via palladium-catalyzed Kumada type coupling of the dibromo compound **2** with 4-pentenylmagnesium bromide as shown in Scheme 1. Ring-closing olefin metathesis of diene **3** was effected in toluene at ∼0.4 mM concentration catalyzed

† Max-Planck-Institute for Polymer Research.
‡ Humboldt University Berlin.
§ New address: Department of Chemistry, University of Kentucky, Lexington, KY 40506-0055.

(1) Ito, S.; Wehmeier, M.; Brand, J. D.; Kübel, C.; Epsch, R.; Rabe, J. P.; Müllen, K. *Chem.-Eur. J.* **2000**, *6*, 4327.
(2) Fleming, A. J.; Coleman, J. N.; Dalton, A. B.; Fechtenkötter, A.; Watson, M. D.; Müllen, K.; Byrne, H. J.; Blau, W. J. *J. Phys. Chem. B* **2003**, *107*, 37−43.
(3) (a) Fischbach, I.; Pakula, T.; Minkin, P.; Fechtenkötter, A.; Müllen, K.; Spiess, H. W.; Saalwächter, K. *J. Phys. Chem. B* **2002**, *106*, 6408. (b) Brown, S. P.; Schnell, I.; Brand, J. D.; Müllen, K.; Spiess, H. W. *J. Mol. Struct.* **2000**, *521*, 179−95.
(4) Stabel, A.; Herwig, P.; Müllen, K.; Rabe, J. P. *Angew. Chem., Int. Ed. Engl.* **1995**, *34*, 303−07.

10.1021/ja037520p CCC: $27.50

Scheme 1. Cyclophane Synthesis[a]

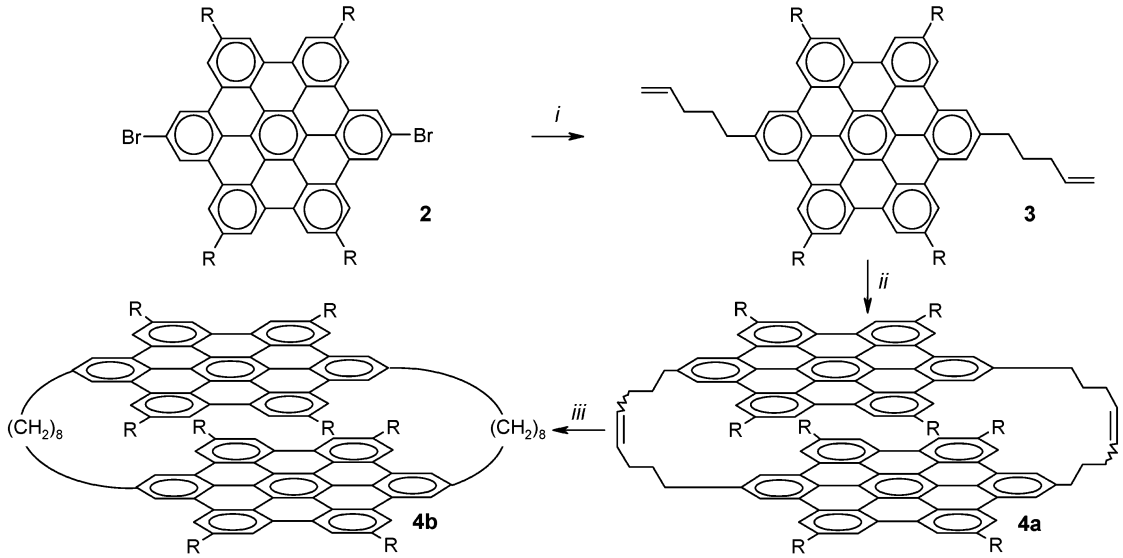

[a] (i) 4-Pentenyl magnesium bromide, PdL_n, THF, 55 °C. (ii) RuL_n, toluene, room temperature. (iii) Pd/C (10%), THF, H_2, room temperature. R = 3,7-dimethyl octanyl.

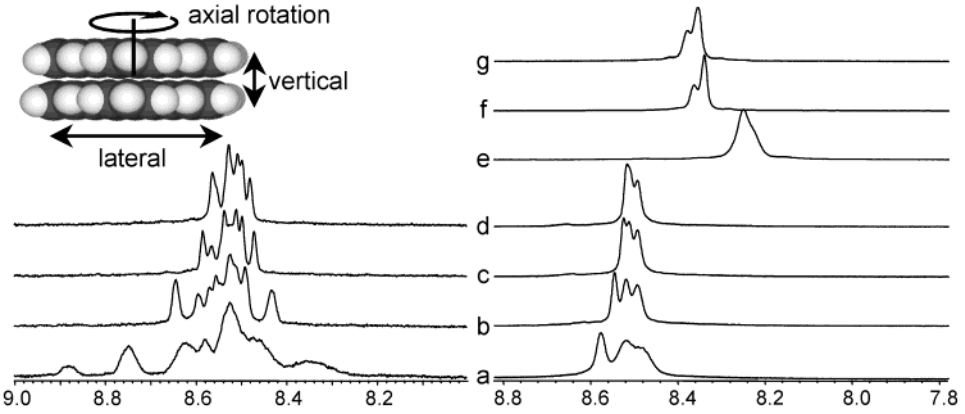

Figure 1. Variable-temperature ^{1}H NMR partial spectra (500 MHz) of cyclophanes **4a**,**b** in *o*-dichlorobenzene-d_4 at (a) 33 °C, (b) 100 °C, (c) 150 °C, (d) 170 °C, and in 1,1,2,2-tetrachloroethane-d_2 at (e) 33 °C, (f) 120 °C, (g) 140 °C. Left, **4a**; right, **4b**. The inset shows the possible intramolecular motions of disks within a cyclophane.

by Grubbs' ruthenium benzylidine [$(PCy_3)_2Cl_2RuCHPh$]. Within 30 min of catalyst addition, the initially yellow solution became turbid. Progress of the olefin metathesis reaction could be followed qualitatively by ^{1}H NMR spectroscopy (ratio terminal/internal olefins, and ethylene) and was virtually complete within 2 h of catalyst introduction. The initial singlet seen for the aromatic-core protons of the monomeric starting material **3** is converted to a progressively broadened distribution of resonances. MALDI-TOF analysis after 48 h reaction time showed the equilibrium product mixture to be largely the desired cyclophane plus smaller amounts of open dimer, trimer, tetramer, etc. Cyclophane **4a** could be separated almost completely from the open oligomers based solely on solubility by passing the cloudy toluene mixture through a 0.45 μm filter. The last traces of oligomers were then removed, according to MALDI and GPC, by passage of the clear yellow filtrate through a short pad of silica gel, giving finally the target macrocycle **4a** in ~64% isolated yield. The olefinic linkages were quantitatively hydrogenated over Pd/C to produce **4b**.

Solution Characterization. Variable-temperature solution ^{1}H NMR spectra (500 MHz) of cyclophanes **4a**,**b** are shown in Figure 1. For cyclophane **4a**, a distribution of resonances from the aromatic-core protons covers a range of 0.6 ppm at room temperature (Supporting Information), but converges with heating, never approaching a single peak even when heated as high as 170 °C. The distribution is much narrower (0.2 ppm, room temperature) for **4b** and nearly completely converges at 170 °C. Solution photoexcitation and emission spectra of **4a**,**b** (Supporting Information) at micromolar concentrations are significantly broadened and almost featureless, but not shifted, relative to model compound **1c**.

Bulk Characterization. When viewed between cross-polars, thin films of **4a**,**b** are birefringent up to their clearing points around 400 °C. From DSC, cyclophane **4a** shows a reversible endothermic first-order transition at 40 °C on heating, while **4b** shows only a very weak second-order transition, most likely a glass transition, at −10 °C. The columnar mesophases were elucidated from 2D WAXD measurements of mechanically extruded fibers,[3a] in which the columnar and fiber axes coincide. A composite of the WAXD fiber diagrams of cyclophane **4a** at room temperature and at 80 °C is shown in Figure 2, and the derived unit cell data from both **4a**,**b** are collected in Table 1.

STM/STS Investigation of Self-Assembled Monolayers. Figure 3 displays the STM current images of monolayers of **4a**

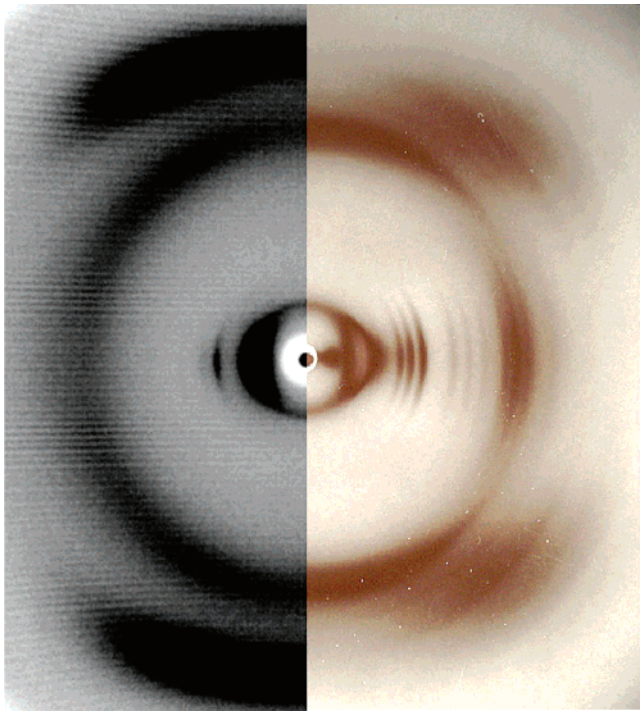

Figure 2. WAXD fiber diagrams of cyclophane **4a** at room temperature (right side) and at 80 °C (left side) from film and CCD cameras, respectively. The film image shown was overexposed to visualize weaker reflections. The smallest angle equatorial reflection in the film image is an artifact ("Bremsstrahlung").

and **4b** physisorbed at the interface between an organic solution and the basal plane of highly oriented pyrolytic graphite (HOPG). Both images reveal monolayers exhibiting epitaxially oriented crystals with point and line defects. Similarly to the case of the corresponding hexaalkylated HBC,[4] the bright spots can be attributed to the π-conjugated cores of the molecules, while dark areas are supposed to be dynamically occupied by alkyl chains. **4a** exhibits a hexagonal packing with a lattice parameter ($a = 1.95 \pm 0.15$ nm) which is indistinguishable from the model HBC **1c**. Very rarely, small domains with a dimer-row arrangement similar to that of **4b** were observed. **4b** exhibits a structure with two molecules per unit cell and parameters $a = (1.81 \pm 0.1)$ nm, $b = (4.07 \pm 0.15)$ nm, and $\alpha = (73° \pm 2°)$. However, in general, the crystalline domains of **4b** were found to be larger and more stable in time than those of **4a**. For this reason, submolecularly resolved STS investigations concentrated on molecules **4b**, with **1b** as reference.

Figure 4 displays averaged current−voltage characteristics (I−V curves) through the aromatic core and the alkyl chain regions of crystalline domains of **1b** and **4b**. Within experimental accuracy (lowest with about 10% at +1.5 V), the I−V's through the aromatic cores of **1b** and **4b** are indistinguishable. For technical reasons, all curves have been recorded at a gap defined by the starting tunneling conditions of −1.4 V sample bias and 500 pA tunneling current. They were then normalized by a constant factor to exhibit the same current at positive sample bias (Figure 4b).

Discussion

Synthesis. Ring-closing olefin metathesis (RCM) is a highly effective method for macrocycle formation from dienes.[5] In molecular systems designed to favor specific intermolecular interactions (H-bonding),[6] for example, sequenced cyclic oligopeptides,[6b,c] excellent to quantitative capture of the desired assemblies from diene-functionalized derivatives has been realized. We were interested in determining if the relatively nonspecific $\pi-\pi$ aggregation of HBC disks, persisting to nanomolar concentrations, could lead to high-yielding intermolecular RCM relying solely on concentration as a controlling factor. We first qualitatively assessed the aggregation behavior of the model compound **1c** by vapor pressure osmometry (VPO, not shown). A plot of the VPO data deviated strongly from linearity, typical for dynamic aggregation.[7] The aggregate number decreases with dilution and was estimated to be between two and three at $10^{-3}-10^{-4}$ M (toluene), which is the concentration range chosen for covalent capture to produce cyclophane **4a**. The result is ∼64% isolated yield, which is excellent when compared to the capture of porphyrin cyclophanes by other chemical pathways.[8]

In addition to RCM, ring-opening metathesis (ROMP) of the cyclophane and acyclic diene metathesis (ADMET) should occur to produce an equilibrium mixture of cyclic and linear species. However, **4a** could be isolated in pure form based solely on its higher solubility. The low solubility of oligomers is attributed to noncovalent network formation (covalently cross-linked noncovalent columns formed through $\pi-\pi$ stacking). Cyclophanes **4a**,**b** are in fact more soluble than monomer **3** as the ratio of available π-surface to solubilizing chains is reduced approximately to one-half.

Cyclophane **4a** is an isomeric mixture with cis−trans olefinic linkages (^{1}H NMR, Supporting Information). For comparison, isomer-free cyclophane **4b** was prepared via reduction of the olefinic bonds with palladium on activated carbon under an atmosphere of hydrogen. As the relative change in mass upon this reduction is extremely small, accurate MALDI is indispensable. Nominal masses and isotopic distributions of the two cyclophanes match those simulated from their molecular formulas (Supporting Information).

Conformational Analysis: Solution Studies. Before evaluating the single-molecule electrical properties of these dyads by scanning probe methods, we proved their intramolecular face-to-face geometries. Solution photoluminescence and excitation spectra of **4a**,**b** in the micromolar concentration range (*o*-dichlorobenzene, Supporting Information) are broadened but not significantly shifted relative to the monomer **1c**, such that the clearly resolved vibrational progression arising from the latter is visible in the spectra of the cyclophanes only as humps. Recent photoluminescence studies[2] revealed that concentrations lower than 10^{-9} M are needed to exclude aggregate formation from **1c**, which explains the small shifts in the spectra of the cyclophanes relative to "monomeric" disks.

(5) (a) Lee, C. W.; Grubbs, R. H. *J. Org. Chem.* **2001**, *66*, 7155−58. (b) Wendland, M. S.; Zimmerman, S. C. *J. Am. Chem. Soc.* **1999**, *121*, 1389−90.
(6) (a) Cardullo, F.; Crego Calama, M.; Snellink-Ruël, B. H. M.; Weldmann, J.-L.; Bielejewska, A.; Fokkens, R.; Nibberling, N. M. M.; Timmerman, P.; Reinhoudt, D. N. *Chem. Commun.* **2000**, 367−68. (b) Clark, T. D.; Kobayashi, K.; Ghadiri, M. R. *Chem.-Eur. J.* **1999**, *5*, 782−92. (c) Clark, T. D.; Ghadiri, M. R. *J. Am. Chem. Soc.* **1995**, *117*, 12364−65.
(7) Tobe, Y.; Utsumi, N.; Kawabata, K.; Nagano, A.; Adachi, K.; Araki, S.; Sonoda, M.; Hirose, K.; Naemura, K. *J. Am. Chem. Soc.* **2002**, *124*, 5350−64.
(8) (a) Tashiro, K.; Aida, T.; Zheng, J.-Y.; Kinbara, K.; Saigo, K.; Sakamoto, S.; Yamaguchi, K. *J. Am. Chem. Soc.* **1999**, *121*, 9477−78. (b) Anderson, H. L.; Hunter, C. A.; Meah, N.; Sanders, J. K. M. *J. Am. Chem. Soc.* **1990**, *112*, 5780−89. (c) Leighton, P.; Cowan, J. A.; Abraham, R. J.; Sanders, J. K. M. *J. Org. Chem.* **1988**, *53*, 733−40.

Table 1. Miller Indices (*hkl*) and *d* Spacings from WAXD of Oriented Fibers of Cyclophanes **4a**,**b**

	(100)	(010)	(110)	(200)	(020)	(210/120)	(300)	(030)	(220/310)	(130)	(400)	(320/230)
4a rt	19.0	17.4	10.8	9.72	8.67	6.91	6.33	5.76	5.19	4.98	4.73	4.29
calc[a]	19.0	17.4	10.8	9.51	8.71	(7.17/6.89)	6.34	5.81	(5.39/5.28)	4.99	4.75	(4.32/4.22)
4a 80 °C	20.8[b]	12.0	10.4									
4b rt	19.9[c]	11.6	10.1									

[a] Calculated for a monoclinic unit cell with $a = 20.98$ Å, $b = 19.22$ Å, $\gamma = 115°$. [b] $a = 24.0$ Å. [c] $a = 23.1$ Å.

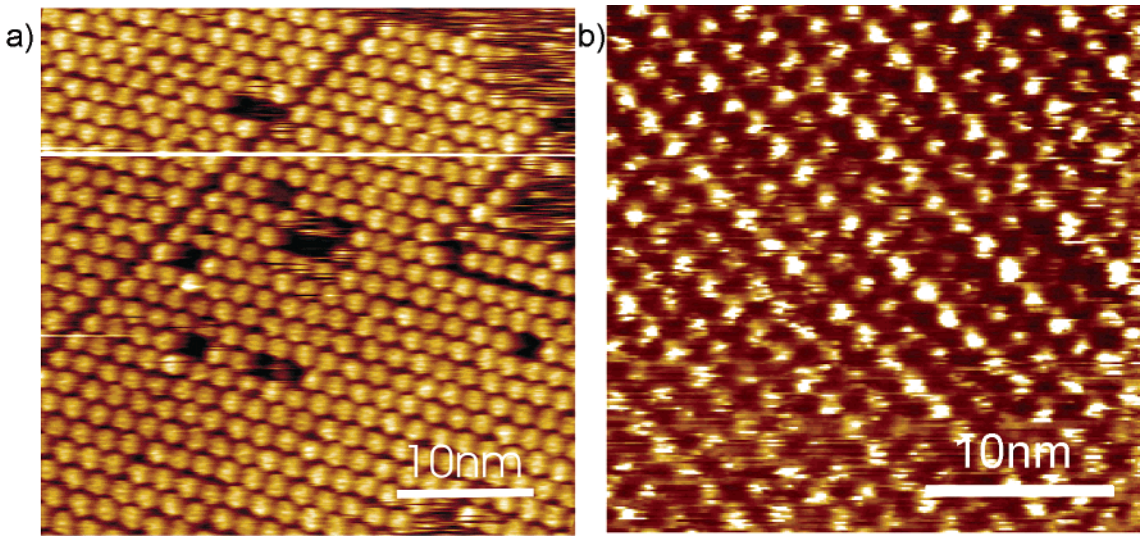

Figure 3. STM images of monolayers at the solution−HOPG interface of (a) **4a** exhibiting a hexagonal packing with a lattice constant $a = 1.95 \pm 0.15$ nm, and (b) **4b** exhibiting unit cell parameters $a = (1.81 \pm 0.1)$ nm, $b = (4.07 \pm 0.15)$ nm, and $\alpha = (73° \pm 2°)$. Tunneling conditions: (a) sample bias $U_s = -1.25$ V, $I_t = 46$ pA; (b) $U_s = -1.4$ V, $I_t = 50$ pA.

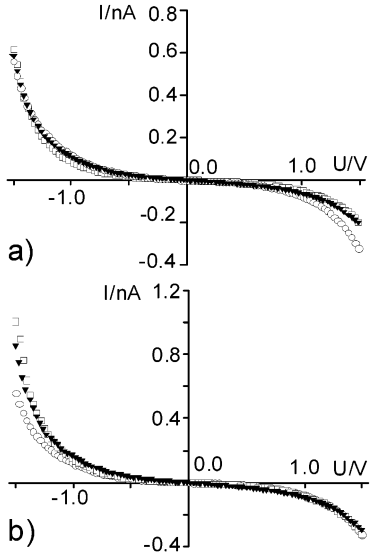

Figure 4. Current−voltage characteristics for aromatic core and alkyl chain regions in crystalline domains of **1b** (open squares □ and open circles ○) and **4b** (black triangles ▼) (a) as measured and (b) normalized to the tunneling barrier impedance of alkyl chain regions for positive sample bias. The curves shown are averaged over 74, 39, and 88 single molecules characteristic of aromatic core regions in crystalline domains of **1b** and **4b** and alkyl chain regions in crystalline domains of **1b**, respectively. The tunneling conditions before switching off the feedback loop were $U_t = -1.4$ V and $I_t = 500$ pA. The vertical dimensions of the symbols approximately reflect the experimental accuracy.

The arrangement of adjacent disks carrying long alkyl chains can vary in a number of ways as portrayed in Figure 1. On average, the two planar disks within a cyclophane should remain separated by ~3.5 Å, dictated by their van der Waals thickness. The proof of face-to-face interaction of the disks within single cyclophanes and insight into its nature were gained from solution ^{1}H NMR spectroscopy, capitalizing on the strong magnetic anisotropy of the aromatic cores to probe local environments.[3] The partial ^{1}H NMR spectra of the aromatic region (Figure 1; full spectra in Supporting Information) show solvent- and temperature-dependent conformational and aggregation behavior.

For comparison, the aromatic core protons of model compound **1c** give rise to a single resonance[9] which shifts with increasing temperature to lower field corresponding to decreasing aggregate number.[10] In contrast, **4a**,**b** show a spread of resonances at room temperature in *o*-dichlorobenzene, which converge on heating toward a value on the high-field side of the middle of the original distribution. The number and spread of peaks cannot be attributed to the substitution pattern, as the aromatic core protons of diene monomer **3** give a single resonance in a number of solvents (THF-d_4, $C_2H_2Cl_4$-d_2, toluene-d_8, *o*-dichlorobenzene-d_4) and temperatures. We attribute this effect to an average lateral offset, on the NMR time scale, of the two disks within cyclophanes as has been reported[8c] for porphyrin cyclophanes. This offset in face-to-face stacked π-systems has been attributed to the drive to reduce $\pi-\pi$ repulsion,[11] which should become energetically more important when mobility is sufficiently decreased.

(9) Fechtenkötter, A.; Tchebotareva, N.; Watson, M.; Müllen, K. *Tetrahedron* **2001**, *57*, 3769−83.
(10) (a) Shetty, A. S.; Zhang, J.; Moore, J. S. *J. Am. Chem. Soc.* **1996**, *118*, 1019. (b) Shetty, A. S.; Fischer, P. R.; Storck, K. F.; Bohn, P. W.; Moore, J. S. *J. Am. Chem. Soc.* **1996**, *118*, 9409. (c) Lahiri, S.; Thompson, J. L.; Moore, J. S. *J. Am. Chem. Soc.* **2000**, *122*, 11315−19.
(11) Hunter, C. A.; Lawson, K. R.; Perkins, J.; Urch, C. J. *J. Chem. Soc., Perkin Trans.* **2001**, *2*, 651−69.

The distribution of resonances from **4a** (0.6 ppm at RT) is larger than that from **4b** (0.2 ppm at RT) at all measured temperatures. The olefinic linkages in the former restrict conformational freedom and in more than one fashion due to cis/trans isomerism (mixture of cis−cis, cis−trans, and trans−trans), leading to a greater number of local environments. The narrower peak distributions upon heating can be attributed to an increase in any of the motions indicated in Figure 1. In $C_2D_2Cl_4$, the core protons of **4b** give rise to only one resonance at room temperature, which shifts downfield on heating and develops a second maximum. We conclude that the cyclophanes **4a**,**b** do not aggregate in *o*-dichlorobenzene at all temperatures measured, but show a temperature-dependent aggregation number in $C_2D_2Cl_4$.

The temperature-dependent spectral changes noted in *o*-dichlorobenzene are similar to solid-state measurements of monomers **1**.[3] In the solid state, a regular lateral displacement within columnar stacks gives rise to a broad range of resonances (>2 ppm) with three maxima. Upon heating to the thermotropic mesophase in which the disks rapidly rotate and their centers of mass coincide along the columnar axes, a single, significantly narrower resonance is observed with a maximum on the high-field side of the center of the original distribution. In solution, substitution of two of the *n*-alkyl chains of **1b** with *tert*-butyl groups results in multiple sharp aromatic proton signals spreading over 1.4 ppm due to lateral displacements to accommodate the bulkier side groups within aggregates.[12] Taking these observations into account, we conclude that the lateral offset of disks within individual cyclophanes **4a**,**b** is not large, considering the relatively narrow spread of core proton resonances (0.6 ppm/**4a**, 0.2 ppm/**4b**).

Bulk Characterization. While our main concern here lies in single-molecule conformations and electrical properties, 2D WAXD measurements of oriented fibers reveal that the bulk self-assembly of cyclophanes **4a**,**b** is not largely altered relative to monomeric disks. Both **4a** (above 40 °C) and **4b** are stacked in columns, arranged in a 2D hexagonal lattice. Hexagonal lateral packing of the columns is clear from equatorial reflections with relative reciprocal spacings of 1, $\sqrt{3}$, and 2 (Figure 2, Table 1). Vertically displaced reflections centered on the meridian at $d \approx 3.6$ Å indicate stacked disks separated by the van der Waals distance typical for alkylated HBCs and no additional repeating elements along the columns. The liquid crystalline nature persists until around 400 °C, as observed by POM.

It should be noted here that the only difference between these two molecules, with masses of $\sim 2.4 \times 10^3$ g/mol, is the presence of unsaturated bonds in the linkages of **4a**. Although **4b** undergoes no phase transitions in addition to its likely glass transition, cooling **4a** below 40 °C causes the disks to tilt relative to the axes of the columns, which themselves rearrange to a primitive monoclinic 2D lattice (cf. Figure 2, Table 1). In the WAXD diffractogram, a hyperbolic set of reflections with vertices on the meridian ($d = 5$ Å) gives a tilt angle of arccos(3.5 Å/5 Å) ≈ 46° relative to the columnar axis, similar to the monomeric **1c**.[13] The off-meridianal reflections indicate 3D correlation (decreased mobility). There is no evidence, for example, additional reflexes along the meridian, or coinciding layer lines, which suggests that the alternating covalent/noncovalent nature of the association in the stacks gives rise to additional periodicity within the columns. It is counterintuitive that conversion of the isomeric mixture (**4a**) to a unique species (**4b**) suppresses crystallization of the rigid mesogenic cores.

STM Investigation of Self-Assembled Monolayers. The images displayed in Figure 3 show evidence that both **4a** and **4b** self-assemble to ordered layers on HOPG, similarly to the corresponding hexaalkylated HBC **1c**.[14] For **4a**, the unit cell is even identical to that of **1c**, hexagonal with the same lattice parameter corresponding to a unit cell area smaller than that of a footprint of the molecule with all side chains extended in all-trans conformations. Accordingly, the alkyl chains must bend up from the surface, and from a comparison of the two areas one can conclude that on average only the aromatic core and the side chains up to the first methyl branch can be oriented parallel to the substrate.[14] Contrary to the bulk behavior noted above, the effect of isomeric purity is reflected in the expected manner in the 2D lateral packing at the solution−graphite interface. Isomerically pure **4b** self-assembles to larger, less defective, and more stable domains. The unit cell exhibits less symmetry with an area per molecule ∼10% larger than that for **4a**, corresponding to all side chains oriented parallel to the substrate.

For the discussion of the STS results, we assume resonantly enhanced tunneling[15] to be the major charge-transfer mechanism. The current−voltage characteristics of the alkyl chain regions are indistinguishable from I−V's of HOPG covered with neat solvent[4] and are supposed to reflect the intrinsic asymmetry of the tunneling junction, which is due to the difference between the two different electrodes, tip and substrate. Within the model of resonant tunneling, this can be explained by the large HOMO−LUMO gap of alkanes which accounts for a very large energetic separation of these levels from the Fermi level of HOPG[16,17] and thus prevents resonant contributions to the tunneling current.

The I−V's of the aromatic regions, on the other hand, exhibit an additional asymmetry when compared to the alkyl chain region curves. According to the resonant tunneling model, molecules that are positioned either spatially or energetically (HOMO and LUMO with respect to the Fermi level of the electrodes at zero bias) symmetrically in the tunneling gap should lead to symmetric I−V's. We therefore conclude that the molecules under study are spatially closer to one of the electrodes and that either the HOMO or the LUMO is closer to the Fermi level of the substrate. In the following, we assume the molecules to be closer to the substrate than to the tip because the monolayer formation indicates a rather strong interaction between molecules and substrate. Furthermore, we assume the Fermi level of the substrate to be in the HOMO−LUMO gap of the molecules at zero bias.

(12) Brand, J. D. *Supramolekulare Strukturen Polycyclischer Aromatischer Kohlenwasserstoffe: Synthese, Charakterisierung, Eigenschaften*; Ph.D. Dissertation, Johannes Gutenberg University; Mainz, Germany, 1999.

(13) (a) Bunk, O.; Nielsen, M. M.; Sølling, T. I.; van de Craats, A. M.; Stutzmann, N. *J. Am. Chem. Soc.* **2003**, *125*, 2252−58. (b) van de Craats, A. M.; Stutzmann, N.; Bunk, O.; Nielsen, M. M.; Watson, M. D.; Müllen, K.; Chanzy, H. D.; Sirringhaus, H.; Friend, R. H. *Adv. Mater.* **2003**, *15*, 495−99.

(14) Samori, P.; Fechtenkötter, A.; Jäckel, F.; Böhme, T.; Müllen, K.; Rabe, J. P. *J. Am. Chem. Soc.* **2001**, *123*, 11462−67.

(15) Mizutani, W.; Shigeno, M.; Kajimura, K.; Ono, M. *Ultramicroscopy* **1992**, *42*−*44*, 236−41.

(16) Willis, R. F.; Feuerbacher, B.; Fitton, B. *Phys. Rev. B* **1971**, *4*, 2441−2452.

(17) Lambin, G.; Delvaux, M. H.; Calderone, A.; Lazzaroni, R.; Brédas, J. L.; Clarke, T. C.; Rabe, J. P. *Mol. Cryst. Liq. Cryst.* **1993**, *235*, 75−82.

In this case, upon the application of a negative sample bias, the HOMO of the molecules shifts up with respect to the Fermi level at the tip and increases the tunneling probability, while at the same time the energetic distance between the LUMO of the molecule and the Fermi level at the tip increases. Thus, we attribute the resonant contributions at negative sample bias to resonantly enhanced tunneling through the HOMO of the molecules. This is in agreement not only with previous work on alkylated HBCs at the graphite−solution interface, but also with double layers of HBC on gold surfaces studied under UHV conditions.[18] In these studies, the HOMO and LUMO were found at −1.4 and +1.8 V sample bias, respectively. Because the accessible bias range is limited by the electrochemistry of the solution, only the onset of the HOMO resonance can be detected, as it is closer to the Fermi level of the substrate than of the LUMO.

The fact that the I−V's through the aromatic regions of **1b** and **4b** do not differ within experimental accuracy is not too surprising. Recent optical studies on functionalized HBCs showed that aggregation affects the optical gap by not more than 0.2 eV.[2] The interaction of a single HBC with a graphite substrate as used in STM/STS experiments may be similar. The possibility that the monolayers of **1b** are in fact double layers and therefore exhibit the same I−V behavior as the related cyclophanes is regarded as very unlikely because, contrary to unsubstituted HBCs,[19] it was not possible to visualize any hypothetical first layer.

Concluding Remarks

The self-assembly, due to $\pi-\pi$ stacking, of hexa-*peri*-hexabenzocoronenes in solution is sufficient to promote covalent capture of large, discrete macrocyclic cyclophanes in good yield under moderate dilution. Solution spectroscopic studies of these cyclophanes indicate a face-to-face intramolecular arrangement of disks with slight lateral displacement at room temperature. The new cyclophanes showed well-defined, columnar discotic phases in the bulk state, which correspond to the arrangement of monomeric disks. That is, the covalent linkages do not cause a measurable variation in the inter- or intramolecular stacking, or the packing of the columns. A very small change in the structure of these large cyclophanes (MW $\approx$ 2400 g/mol), that is, saturation of two olefin bonds in the chains connecting the two faces, suppressed the bulk crystallization of the rigid cores, while it lowers the symmetry of the crystalline packing in monolayers at the solution−graphite interface. In STS, no significant change for the cyclophanes in comparison to the reference monomeric molecules was observed. After demonstrating the feasibility of STM and STS studies on cyclophanes with large aromatic constituents, it would be particularly interesting to compare the current−voltage characteristics for related cyclophanes, where one of the two disks is chemically modified to shift its LUMO and HOMO. This should allow the assembly of arrays of "face-on", in comparison to the classical "end-to-end", donor−acceptor molecules proposed by Aviram and Ratner[20] for molecular diodes. Furthermore, STS measurements of covalent double- or multilayers at the solid−liquid interface open new perspectives in the study of the formation and electronic nature of molecular complexes, for example, before and after intercalation of electron/charge acceptor components,[21] which might be interchanged in a controlled manner based on differing binding constants.

Acknowledgment. This work was supported by EU projects SISITOMAS, DISCEL (Contract G5RD-CT2000-00321), and MAC-MES, the Volkswagen-Stiftung (Elektronentransport durch konjugierte molekulare Scheiben und Ketten), the European Science Foundation through SMARTON, and the German "Bundesministerium für Forschung und Technologie" as part of the program "Zentrum für multifunktionelle Werkstoffe und miniaturisierte Funktionseinheiten" (BMBF 03N 6500).

Supporting Information Available: Full synthetic and experimental details; solution ^{1}H NMR, photoluminescence, and excitation spectra (PDF). This material is available free of charge via the Internet at http://pubs.acs.org.

JA037520P

(18) Törker, M.; Fritz, T.; Pröhl, H.; Gutierrez, R.; Grossmann, F.; Schmidt, R. *Phys. Rev. B* **2002**, *65*, 245422.
(19) Samorí, P.; Severin, N.; Simpson, C. D.; Müllen, K.; Rabe, J. P. *J. Am. Chem. Soc*. **2002**, *124*, 9454−9457.
(20) Aviram, A.; Ratner, M. A. *Chem. Phys. Lett.* **1974**, *29*, 277−283.
(21) Preliminary solution ^{1}H NMR studies indicate that cyclophane **4b** binds (green complex) tetranitrofluorenone (TNF) more strongly than does the monomeric **1c**.